

Quench dynamics and non equilibrium phase diagram of the Bose-Hubbard model

Corinna Kollath,¹ Andreas M. Läuchli,² and Ehud Altman³

¹Université de Genève, 24 Quai Ernest-Ansermet, CH-1211 Genève, Switzerland

²Institut Romand de Recherche Numérique en Physique des Matériaux (IRRMA), CH-1015 Lausanne, Switzerland

³Department of Condensed Matter Physics, The Weizmann Institute of Science, Rehovot 76100, Israel

(Dated: February 6, 2008)

We investigate the time evolution of correlations in the Bose-Hubbard model following a quench from the superfluid to the Mott insulator. For large values of the final interaction strength the system approaches a distinctly non-equilibrium steady state that bears strong memory of the initial conditions. In contrast, when the final interaction strength is comparable to the hopping, the correlations are rather well approximated by those at thermal equilibrium. The existence of two distinct non-equilibrium regimes is surprising given the non-integrability of the Bose-Hubbard model. We relate this phenomenon to the role of quasi-particle interactions in the Mott insulator.

PACS numbers: 03.75.Lm 05.70.Ln 67.40.Fd73.43.Nq

Recent experiments with ultra cold atomic gases have opened exciting possibilities for studying non-equilibrium quantum dynamics of many body systems. In particular, the high degree of tunability allows one to rapidly change system parameters and observe the subsequent quantum evolution. Furthermore, thanks to the almost perfect isolation of the atoms from the environment, the quantum dynamics can remain coherent for exceedingly long times. These advantages were used, for example, to study non adiabatic dynamics across the quantum phase transition between a superfluid and a Mott insulator [1, 2], as well as the crossover of paired fermion superfluids from weak to strong coupling [3, 4].

In many cases the system parameters are changed so fast, that one may consider the sudden limit: The system is prepared in the ground state of an initial Hamiltonian H_i , and then evolves under the influence of a different Hamiltonian H_f . Fundamental questions that arise concern the approach of the system to a new steady state and the nature of this steady state. Does it retain memory of the initial state? How is it related to the thermal equilibrium of H_f ? These questions were addressed in a number of recent works, by solving various integrable models [5, 6, 7, 8, 9, 10]. In these systems the long time steady state was found to be non thermal and often carried memory of the initial state. In a fascinating experiment, Kinoshita *et al.* [11] investigated the thermalization of strongly interacting ultra cold atoms in a *nearly* integrable situation. The result, at the maximal time scale of the experiment, was a non thermalized steady state.

In this Letter we numerically investigate the evolution of correlations following a sudden change of parameters in the *non-integrable* Bose Hubbard model (BHM) [12], describing cold atomic gases in optical lattices [13, 14]

$$H = -J \sum_{\langle i,j \rangle} (b_i^\dagger b_j + h.c.) + \frac{U}{2} \sum_i n_i(n_i - 1). \quad (1)$$

In equilibrium at integer filling, this model exhibits a

quantum phase transition at a critical value of the interaction strength $U/J = u_c$, between a superfluid ($U/J < u_c$) and a Mott insulating state ($U/J > u_c$) [12]. In a one-dimensional system with unit filling $u_c^{1D} \approx 3.37$ [15] and in two dimensions $u_c^{2D} \approx 16.7$ [16].

Our study is motivated by the experiment with ultra cold bosonic atoms in an optical lattice [2], where the lattice intensity was increased suddenly, taking the system from the superfluid phase into the Mott insulator regime. Following the quench, a remarkable series of collapse and revivals of the interference pattern was observed, which relaxed after a few oscillations. What processes are responsible for the relaxation and what is the nature of the steady state that is reached? The general expectation for non-integrable models like (1) is that the long time steady state will be essentially equivalent to thermal equilibrium. Surprisingly, we find that this is not always the case. When the interaction U_f in the final state is much larger than J the system reaches a quasi-steady state that is very different from thermal equilibrium and retains memory of the initial state. As U_f decreases the nature of the steady state changes, and in the region where U_f is comparable to J the steady state correlations are well approximated by those at thermal equilibrium (cf. Fig. 4). We relate this crossover in the non-equilibrium behavior to the ineffectiveness of quasi-particle interactions in the strongly interacting regime.

The revivals seen in the interference patterns in the experiment [2] are easy to understand in the limit $J \rightarrow 0$. In this limit the evolution operator is site factorizable and given by $\prod_i e^{iU_f n_i(n_i-1)t/2}$. This implies periodic time dependence, since the operator $n_i(n_i-1)/2$ takes integer values for any Fock state. An arbitrary initial wave function therefore revives entirely after times $\tau_n = 2\pi n/U_f$ where n is integer (\hbar is set to unity throughout). A non vanishing hopping matrix element J greatly complicates the time evolution, and leads to a relaxation of the oscillations. In the following we investigate this situation using numerical methods and then interpret the

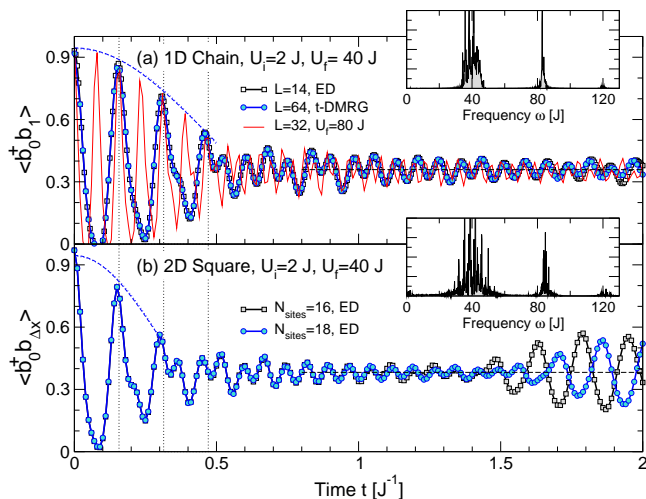


FIG. 1: (Color online) Short time behaviour of the nearest-neighbor correlation functions for $U_i = 2J$ and $U_f = 40J$. (a) t-DMRG and ED results for 1D chains. For comparison the thin full line without symbols shows a relaxation for $U_f = 80J$. (b) ED results for 2D square lattices. In both cases there are clear oscillations with a period $2\pi/U_f$ (dotted vertical lines for $U_f = 40J$), which relax on a time scale of $1/J$. Revival of the correlations at $\approx 1.5/J$ in (b) is due to finite size effects. The two insets show the Fourier transform of the oscillations. The main weight lies in a broad band at $\omega \approx U_f$, with some smaller bands at higher multiples of U_f .

results within a tractable effective model. We implement the dynamic transition from the superfluid to the Mott-insulating regime at unit filling ($n = 1$) by a sudden quench of the interaction U at fixed hopping J . Thus the initial "superfluid" wavefunction is the ground state of the Hamiltonian H_i with $U = U_i < U_c$, and it evolves subject to the Hamiltonian H_f with U_f in the Mott insulator regime or close to the critical point. The time evolution of the many-body wavefunction is computed by exact diagonalization (ED) based on Lanczos-type methods [17, 18] and by the adaptive time-dependent density matrix renormalization group method (adaptive t-DMRG) [19, 20, 21]. The ED is used to study 1D and 2D systems with up to 18 sites, while the adaptive t-DMRG is used for 1D systems with up to 64 sites keeping up to 200 DMRG states. For computational reasons the Hilbert space on each site was truncated at high occupation numbers. In ED (t-DMRG) we typically kept up to 4 (9) bosons per site.

For a sudden quench deep into the Mott-insulating regime we find that a partial revival of the wave-function survives. This can for example be seen in the off-diagonal correlation functions $\langle b^\dagger(x, t)b(0, t) \rangle$ which display oscillations with a period set by $2\pi/U_f$. The oscillations relax to a quasi-steady state on a time scale $\sim 1/J$. We find that this relaxation time, as well as the value of the correlation reached in the quasi-steady state, are independent of U_f for sufficiently large U_f . Fig. 1 shows an example

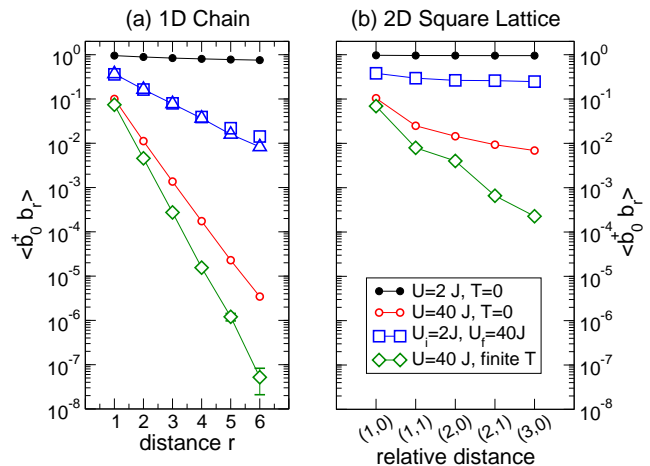


FIG. 2: (Color online) Decay of the correlations $\langle b_i^\dagger b_{i+r} \rangle$ with distance r after a quench from $U_i = 2J$ to $U_f = 40J$. Squares (ED) and triangles (t-DMRG) show the averaged results of the quasi steady state. The average value is determined fitting a linear function to the results between $t_1 \approx J^{-1}$ and $t_2 = 20J^{-1}$. Diamonds show equilibrium QMC results at finite temperature (see text for details), and the filled and open circles display the $T = 0$ correlations in the ground state for U_i and U_f , respectively.

of the evolution of nearest neighbor correlations. A similar evolution is observed for longer range correlations. Later we use a simple model valid at strong coupling to show that the relaxation time is related to the existence of a quasi-particle band of width $\sim J$ around an energy U_f . The short range correlations oscillate with all the frequencies in this band, and therefore they dephase after a time scale of the order of the inverse band width. Indeed a Fourier decomposition of the oscillations (inset of Fig. 1) reveals this band, as well as weaker contributions from higher multiples of U_f . The amplitude of the oscillations with frequencies of higher multiples depends strongly on the particle distribution of the initial state.

We turn to investigate the nature of the quasi-steady state reached by the off-diagonal correlations. The general expectation in non-integrable systems, is that the correlations relax to thermal equilibrium. The temperature at this equilibrium is set by the internal energy imposed on the system by the initial conditions. Interestingly, in spite of the non-integrability of the BHM we find two different regimes of behavior depending mostly on the magnitude of the interaction strength in the final state. When U_f is very large the correlations in the steady state bear strong memory of the initial state. In particular their decay with distance is much slower than the corresponding thermal correlations and even slower than the ground state correlations at the final point. This behavior is shown in Fig. 2. The equilibrium finite temperature correlations were calculated using quantum Monte Carlo (QMC) simulations of the BHM (1) with $U = U_f$, where the temperature was determined

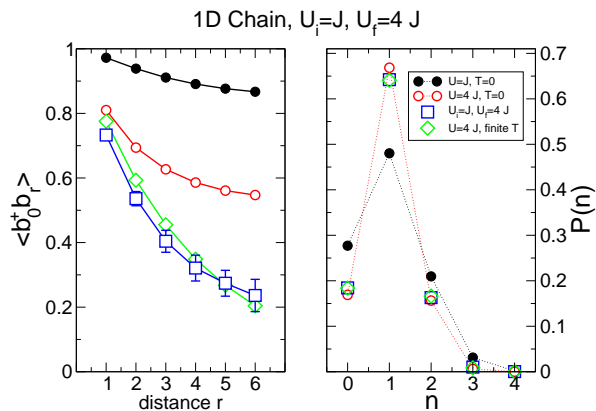


FIG. 3: (Color online) Left panel: Decay of the correlations $\langle b_i^\dagger b_{i+r} \rangle$ with distance r after a quench from $U_i = J$ to $U_f = 4J$. Squares show the averaged results for times between $t_1 \approx J^{-1}$ and $t_2 = 20J^{-1}$ determined as in Fig. 2. Diamonds show equilibrium QMC results at finite temperature ($T \approx 0.8J$) and $U = 4J$, and the filled and open circles display the $T = 0$ correlations in the ground state for U_i and U_f , respectively. Right panel: Particle number distribution $P(n)$. The labeling is the same as in the left panel.

by matching the on-site particle distribution $P(n)$. This yielded $T_{1D} \approx 21.5J$ and $T_{2D} \approx 23.3J$. A completely different regime is realized when the final state is closer to the superfluid transition, i.e. $U_f \lesssim 6J$. In that case the correlations at long times do decay with distance faster than the ground state correlations and fit reasonably well to correlations at thermal equilibrium as calculated using QMC. The good fit of the nearest-neighbor correlations implies together with the matching of the particle distribution that the temperature used for the QMC simulations corresponds to the energy forced into the system by the quench. An example of the correlations in this regime is displayed in the left panel of Fig. 3. Contrary to the regime of large U_f , the oscillations with period $2\pi/U_f$ are overdamped. We note however that in this regime the correlations do not reach a true steady state within the time-scale we are able to simulate reliably.

In contrast to the rich behavior of the off diagonal correlations, on-site quantities such as the particle distribution $P(n)$ reach a much simpler steady state for all U_f we considered. For large U_f , $P(n)$ almost does not relax from the values in the initial state, in agreement with mean-field calculation for the case of high fillings [22]. For smaller U_f some relaxation occurs, see right panel of Fig. 3. In all cases we were able to determine a temperature where the QMC simulations at U_f reproduce the long-time behavior of $P(n)$ to good accuracy.

The essential results of the calculations in different parameter regimes are summarized in Fig. 4. The left panel presents a non-equilibrium phase diagram in the plane of U_i/J and U_f/J . In one region (large U_f) off-diagonal correlations reach a distinctly non thermal steady state.

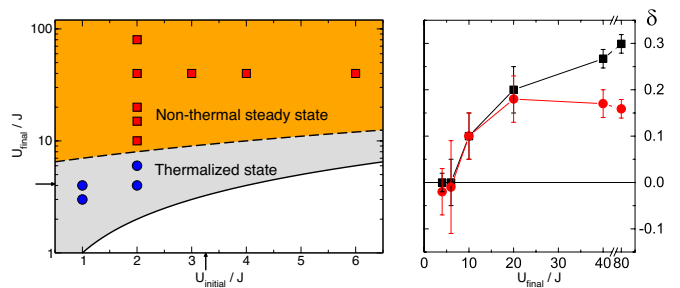


FIG. 4: (Color online) Left panel: Non equilibrium phase diagram in the space of initial and final interaction strengths. Two regions are found, one where the steady state is distinctly non thermal and the other where correlations do appear to thermalize within the numerical error bounds. Squares and circles mark points in the respective regions where numerical results for a one-dimensional system were obtained. The full line follows $U_i = U_f$. Small arrows mark the equilibrium critical value for an infinite one-dimensional system. Right panel: Difference between the correlation $\langle b_i^\dagger b_{i+r} \rangle$ at steady state and its nominal value for the ground state of the final Hamiltonian. Data is shown for $r = 1$ (circles) and $r = 2$ (squares) along the cut $U_i/J = 2$. The crossover from slower than ground state decay ($\delta > 0$) to faster than ground state decay (as expected of thermal correlations) at $U_f \approx 6J$.

In the other region, the correlations after some time, are well described by the thermal equilibrium results. A cut along the line $U_i/J = 2$ shows a clear crossover of the steady state correlations from decaying slower than ground state correlations at U_f to faster than ground state (as expected of thermal correlations) at $U_f \approx 6J$.

We now argue that the different steady state regimes may be understood qualitatively based on a simple model [23]. One can think of the excitations of a Mott insulator as particles and holes (p_i^\dagger and h_i^\dagger) that hop on the lattice and may be created and annihilated in pairs. From this point of view, the initial state (a commensurate superfluid) is a simultaneous condensate of particles and holes. Its time dependence is determined by the effective Hamiltonian in the Mott regime. Neglecting quasi-particle interactions, this Hamiltonian is diagonalized by a Bogoliubov transformation, so that $H_0 = \sum_{\mathbf{k}, \alpha} \omega_{\mathbf{k}} \beta_{\alpha \mathbf{k}}^\dagger \beta_{\alpha \mathbf{k}}$, where $\beta_{\alpha \mathbf{k}}^\dagger$ creates a quasi-particle of the Mott insulator.

Now consider the time evolution of the momentum distribution $\langle n_{\mathbf{k}} \rangle = \langle b_{\mathbf{k}}^\dagger b_{\mathbf{k}} \rangle$. In terms of the particles and holes, a boson is given roughly by the combination $b_{\mathbf{k}}^\dagger \sim p_{\mathbf{k}}^\dagger + h_{-\mathbf{k}}$. Therefore the component $\langle n_{\mathbf{k}}(t) \rangle$ of the momentum distribution can be constructed from quasi-particles of the Mott insulator carrying momenta \mathbf{k} and $-\mathbf{k}$, and it oscillates at a frequency $\omega_{\mathbf{k}}$. This fact bears on the dynamics of spatial correlations $\langle b_{j+r}^\dagger b_j \rangle$, which are the Fourier transform of $\langle n_{\mathbf{k}} \rangle$. Short range correlations receive contributions from all \mathbf{k} components, and therefore they dephase at a rate comparable to the full quasi-particle bandwidth. Long range correlations on the

other hand are dominated by $n_{\mathbf{k}}$ at small k .

Within this picture thermalization occurs due to quasi-particle interactions. In particular the quasi-particle population equilibrates because of quartic processes of the form $\beta_{\mathbf{q}}^{\dagger}\beta_{\mathbf{k}+\mathbf{q}/2}\beta_{-\mathbf{k}+\mathbf{q}/2}\beta_0$. Note that quartic terms that conserve the quasi-particle number cannot by themselves induce thermalization because they do not change the non-equilibrium quasi-particle population forced on the system by the initial conditions. At the level of Fermi's golden rule, the process mentioned above may occur only while conserving energy. But this is impossible deep in the Mott insulator, as long as the gap Δ is larger than half the quasi-particle bandwidth $W \sim 4zJ$. We conclude that thermalization should be effectively suppressed in the regime $U \gg J$, in agreement with the numerical results. Of course there are higher order processes that may still induce thermalization, but apparently this occurs at time scales much larger than the relaxation time $1/J$. On the other hand, as the final state approaches the critical point $\Delta = 0$, quasi-particle interactions become increasingly effective, which leads to rapid thermalization. The simple picture outlined above is strictly valid only for a dilute quasi-particle population, that is for initial state close to the transition. However from the numerical results it seems to apply more generally.

The results of the present study leave open interesting conceptual questions. Is the non thermal state reached a true steady state? Is there a longer time scale associated with reaching true equilibrium as in the prethermalized states discussed in Ref. [24], or a scale free relaxation analogous to aging phenomena?

We propose that some of these questions may be addressed by experiments with ultra cold atoms on optical lattices. The simplest observable to consider is the visibility of the interference pattern as defined in [2]. For example, in a one dimensional homogenous tube, following a quench from $U_i = 2J$ to $U_f = 40J$ we expect, based on t-DMRG calculation, that the visibility will relax to a value of approximately 60%, compared to visibility of only 20% in the ground state of the system with $U = U_f$.

An obstacle for the interpretation of experiments is the existence of additional sources of relaxation, most prominently the confining potential and the presence of many parallel tubes. We performed time dependent Gutzwiller calculations to compare the effect of the confining potential to that of tunneling. The effect of the tunneling dominates, if the energy difference between neighbouring site $V_0(2j - 1)$ is smaller than the width of the particle-hole energy bands $\sim 6zJ$, i.e. $V_0(2j_m - 1)/(6zJ) \lesssim 1$. Here V_0 is the prefactor of the trapping potential and j_m is the extension of the condensate. Substituting into this analysis the experimental parameters of [2] it follows that

the main source of dephasing in that experiment was the confining potential. However it is not difficult to reach the regime where the tunneling gives the dominant contribution.

We thank B. Altshuler, E. Demler, T. Giamarchi, S. Kehrein, S. Manmana, A. Muramatsu, R. Noack, F. Werner, and S. Wessel for fruitful discussions. This work was partly supported by the SNF under MaNEP and Division II, and by the DFG grant HO 2407/2-1. EA acknowledges support of the U.S.-Israel binational science foundation. We acknowledge the allocation of computing time at CSCS (Manno) and LRZ (Garching). The QMC simulations have been performed using the SSE application [26, 27] of the ALPS project [28?].

-
- [1] M. Greiner, *et al.*, Nature **415**, 39 (2002).
 - [2] M. Greiner, *et al.*, Nature **419**, 51 (2002).
 - [3] M. Greiner, *et al.*, Phys. Rev. Lett. **94**, 070403 (2005).
 - [4] M.W. Zwierlein, *et al.*, Phys. Rev. Lett. **94**, 180401 (2005).
 - [5] F. Iglói and H. Rieger, Phys. Rev. Lett. **85**, 3233 (2000).
 - [6] K. Sengupta, *et al.*, Phys. Rev. A **69**, 053616 (2004).
 - [7] R. W. Cherng and L. S. Levitov, Phys. Rev. A **73**, 043614 (2006).
 - [8] P. Calabrese and J. Cardy, Phys. Rev. Lett. **96**, 136801 (2006).
 - [9] M. Rigol, *et al.*, Phys. Rev. Lett. **98**, 050405 (2007).
 - [10] M. Cazalilla, Phys. Rev. Lett. **97**, 156403 (2006).
 - [11] T. Kinoshita *et al.*, Nature **440**, 900 (2006).
 - [12] M. P. A. Fisher, *et al.*, Phys. Rev. B **40**, 546 (1989).
 - [13] D. Jaksch, *et al.*, Phys. Rev. Lett. **81**, 3108 (1998).
 - [14] W. Zwerger, Journal of Optics B: Quantum Semiclass. Opt. **5**, S9 (2003).
 - [15] T. Kühner, *et al.*, Phys. Rev. B **61**, 12474 (2000).
 - [16] N. Elstner and H. Monien, Phys. Rev. B **59**, 12184 (1999).
 - [17] T.J. Park and J.C. Light, J. Chem. Phys. **85**, 5870 (1986).
 - [18] S. R. Manmana, *et al.*, AIP Conf. Proc. **789**, 269 (2005).
 - [19] S.R. White and A.E. Feiguin, Phys. Rev. Lett. **93**, 076401 (2004).
 - [20] A.J. Daley *et al.*, J. Stat. Mech.: Theor. Exp. **P04005** (2004).
 - [21] D. Gobert *et al.*, Phys. Rev. E **71**, 036102 (2005).
 - [22] R. Schützhold, *et al.*, Phys. Rev. Lett. **97**, 200601 (2006).
 - [23] E. Altman and A. Auerbach, Phys. Rev. Lett. **89**, 250404 (2002).
 - [24] J. Berges, *et al.*, Phys. Rev. Lett. **93**, 142002 (2004).
 - [27] F. Alet, *et al.*, Phys. Rev. E **71**, 036706 (2005).
 - [26] A. W. Sandvik, Phys. Rev. B **59**, R14157 (1999).
 - [27] A.F. Albuquerque *et al.*, J. Magn. Mag. Mat. **310**, 1187 (2007).
 - [28] M. Troyer, B. Ammon, and E. Heeb, Lecture Notes in Computer Science **1505**, 191 (1998).